First-passage time in a bistable potential with colored noise

Laureano Ramirez-Piscina and José María Sancho

Department d'Estructura i Constituents de la Materia, Facultat de Física, Universitat de Barcelona,
Diagonal 647, 08028 Barcelona, Spain

F. Javier de la Rubia

Física Fundamental, Universidad Nacional de Educación a Distancia, Apartado de Correos 60141, 28071 Madrid, Spain

Katja Lindenberg and George P. Tsironis*

Department of Chemistry, B-040, and Institute for Nonlinear Science, R-002,
University of California–San Diego, La Jolla, California 92093

(Received 6 April 1989)

A precise digital simulation of a bistable system under the effect of colored noise is carried out. A set of data for the mean first-passage time is obtained. The results are interpreted and compared with presently available theories, which are revisited following a new insight. Discrepancies that have been discussed in the literature are understood within our framework.

I. INTRODUCTION

A number of (sometimes conflicting) views have recently dominated the literature on bistable processes driven by external noise. Most of the conflicts arise in the context of the effects of external noise that is colored, e.g., whose correlations decay exponentially with a correlation time $\tau > 0$. Varous theoretical approaches have been developed in the small-τ (Refs. 1–7) and in the large-τ (Refs. 7–10) limits, and some of the predictions emerging from these theories have been tested against analog simulations,[2] numerical computations,[11,12] and a few numerical (digital) simulations.[1,13,14]

In order to attain a better understanding of the relations among these various theories and the accuracy of their predictions, we have carried out extensive numerical simulations of the Langevin equations that serve as the model from which all these theories depart. By covering extensive ranges of parameter values (in particular, of the correlation time τ of the noise), we are able to arrive at some definitive conclusions that should help to sort out some of the present uncertainties in the field. It should be remarked that the main contribution of this paper lies not in the accuracy of the computer simulations (which is comparable to that of other recent simulations[13]) but in the insight and better understanding of the present theories acquired through the data.

As our system we shall consider the generic and widely studied bistable system

$$\dot{q}(t) = q(t) - q^3(t) + \mu(t) , \tag{1.1}$$

where $\mu(t)$ is the noise driving the system, which we shall assume to be Gaussian throughout this analysis. In the absence of the noise, the system has fixed points at $q = \pm 1$ (stable) and at $q = 0$ (unstable). If $\mu(t)$ represents white noise, then its correlation function is

$$\langle \mu(t)\mu(t') \rangle = 2D\delta(t - t') . \tag{1.2}$$

If the noise is Gaussian colored, then

$$\langle \mu(t)\mu(t') \rangle = \frac{D}{\tau} e^{|t-t'|/\tau} . \tag{1.3}$$

The colored noise can itself be generated from a white noise process $\mu_w(t)$ via the dynamical equation

$$\dot{\mu}(t) = -\frac{1}{\tau}\mu(t) + \frac{1}{\tau}\mu_W(t) . \tag{1.4}$$

Herein we consider two quantities most frequently discussed in the literature: the mean first-passage time (MFPT) for the system starting from one well of the bistable potential, e.g., at $q = -1$, to reach $q = 0$ (T_{top}) or to cross the barrier and reach the other potential well, e.g., at $q = 1$ (T_{bot}). A third time of interest that we consider is the MFPT to reach the separatrix between the wells (T_{sep}).

Considerable discussion has recently centered on the appropriate (meaningful) end points to use in MFPT calculations since the fixed points in the absence of the noise are instantaneously shifted by the (colored) noise, and especially since $q = 0$ is not the separatrix between the two potential wells in the presence of (colored) noise. Thus, whereas it is generally agreed upon that T_{bot} does represent a transition time from one well to the other (even in the face of shifting minima), T_{top} is only an accurate measure of this transition when the noise is white and D is small, and T_{sep} is only an accurate measure of T_{bot} when D is small. These remarks notwithstanding (and we shall return to this issue later), we will use these three quantities to asses the validity of various theories because they have been so prominent in the literature. Quite aside from the physical content of these measures they can of course still be used to compare analytic theories with simulations.

For white noise the MFPT can be expressed exactly as a double integral[3,15] that can then be evaluated by numer-

ical procedures. When a steepest descent approximation is applied to these integrals, one obtains analytic estimates ("Kramers times"[16]) for T_{top}^K and T_{bot}^K,

$$T_{top}^K = \frac{\pi}{\sqrt{2}} e^{1/4D} \qquad (1.5)$$

and

$$T_{bot}^K = \pi\sqrt{2} e^{1/4D} . \qquad (1.6)$$

These results, valid only in the "high-barrier" asymptotic limit $D \to 0$, reflect the fact that upon reaching the top of the barrier half of the trajectories immediately go on to the new well while the other half return to the original well. For finite D Larson and Kostin[17] have calculated the first correction to these results. This correction reads

$$T^{LK} = (1 + \tfrac{3}{2}D)T^K . \qquad (1.7)$$

There exist no exact analytic results (or even analytic results in the form of integral expressions) when the noise driving the system is colored. A number of approximate theories have been developed, all of them dealing with the limiting cases of either very short or very long correlation time of the noise. The small-τ theories arrive at expressions similar to (1.5) and (1.6) with corrections that contain a τ dependence. The long-τ theores arrive at expressions that are quite different from the white-noise results. In the first (small-τ) group the following expressions have appeared in the literature:

$$T_{top}(\tau) = \frac{\pi}{\sqrt{2}} \left[\frac{1+2\tau}{1-\tau} \right]^{1/2} e^{1/4D} , \qquad (1.8)$$

$$T_{top}(\tau) = \frac{\pi}{\sqrt{2}} e^{1/4D + (3/2)\tau} , \qquad (1.9)$$

$$T_{sep}(\tau) = \frac{\pi}{\sqrt{2}} \frac{(1-2\tau+\tau^2)^{1/2}}{(1+4\tau+4\tau^2)^{1/2}} \frac{1+3\tau+\tfrac{5}{2}\tau^2}{1-\tfrac{3}{2}\tau+\tfrac{5}{8}\tau^2}$$

$$\times \exp\left[\frac{1}{D} \left[\frac{1}{4} + \frac{\tau^2}{8} - \frac{3\tau^4}{10} \right] \right] , \qquad (1.10)$$

$$T_{top}(\tau) = \frac{\pi}{\sqrt{2}} \left[1 - \left[\frac{2}{\pi} \right]^{1/2} \zeta(\tfrac{1}{2})\sqrt{\tau} + \tfrac{3}{2}\tau \right] e^{1/4D} . \qquad (1.11)$$

Equation (1.8) was derived by Hänggi, Marchesoni, and Grigolini,[1] and Fox;[5] Eq. (1.9) was obtained by Masoliver, West, and Lindenberg;[3] Eq. (1.10) is the MFPT to the separatrix derived by Klosek-Dygas Matkowsky, and Schuss;[6] Eq. (1.11) [with $\zeta(\tfrac{1}{2}) = -1.460354\ldots$] is due to Doering, Hagan, and Levermore.[4]

An approximation for T_{bot} valid for small D but for arbitrary correlation times τ was proposed by Luciani and Verga.[17] Their "interpolation formula" [Eq. (66) of Ref. 7], applied to our system, is

$$T_{bot}(\tau) = \pi\sqrt{2}(1+3\tau)^{1/2} \exp\left[\frac{1}{4D} \frac{1+\tfrac{27}{16}\tau+\tfrac{1}{2}\tau^2}{1+\tfrac{27}{16}\tau} \right] . \qquad (1.12)$$

For very large τ the following approximations have been published:

$$T(\tau) = \left[\frac{\pi}{\sqrt{2}} + \left[\tfrac{27}{2}\pi D\tau \right]^{1/2} e^{2\tau/27D} \right] e^{1/4D} , \qquad (1.13)$$

$$T(\tau) = [27\pi D(\tau+\tfrac{1}{2})]^{1/2} \exp\left[\frac{2\tau}{27D} + \frac{1}{9D} \right] . \qquad (1.14)$$

Equation (1.13) was obtained by Tsironis and Grigolini[8] and is designed to bridge the $\tau \to 0$ and $\tau \to \infty$ results. Equation (1.14) is due to Hänggi, Jung, and Marchesoni.[9]

It should be noted that the small-τ expressions (1.8) and (1.9) are to be interpreted not as representing T_{top} but rather $T_{bot}/2$. These two quantities are only equal for white noise and in the weak-noise limit, where $q = 0$ is actually the separatrix between the two wells and where the trajectories reaching this value immediately proceed to one well (half) or the other (the other half). The theory of Doering et al.[4] incorporates finite-τ subtleties that arise from the fact that $q = 0$ is no longer the separatrix and results in the $\sqrt{\tau}$ contribution evident in (1.11). It has been argued[18] (and agreed to by Doering et al.[19]) that a more physical characterization of the transition process is the time to reach the actual separatrix (or the other well), and in this latter calculation [cf. (1.10)] there appear no $\sqrt{\tau}$ contributions.

All the small-τ theories with the exception of Eq. (1.11) thus predict a leading behavior of the form

$$\frac{T_{bot}(\tau)}{T_{bot}(0)} \approx 1 + \tfrac{3}{2}\tau , \qquad (1.15)$$

whereas Doering et al.[4] predict the leading behavior

$$\frac{T_{top}(\tau)}{T_{top}(0)} \approx 1 - \left[\frac{2}{\pi} \right]^{1/2} \zeta(\tfrac{1}{2})\sqrt{\tau} + \tfrac{3}{2}\tau , \qquad (1.16)$$

thus exhibiting the $\sqrt{\tau}$ correction mentioned above.

The large-τ theories [Eqs. (1.13) and (1.14)] and the interpolation formula (1.12) all have the same leading exponential dependence $2\tau/27D$, which is exact in the limit $\tau \to \infty$. The theories differ from one another in their predictions of the behavior at large but finite τ.

II. NUMERICAL ALGORITHMS

The numerical integration of Eq. (1.1) with Gaussian noise $\mu(t)$ of correlation properties (1.2) or (1.3) has been carried out following the procedure detailed in Ref. 20. We have simulated a number of trajectories (typically 500 or 1000) for each choice of parameter values, each driven by a different realization of the noise.

For the case of white noise, the discrete version of Eq. (1.1) is

$$q(t+h) = q(t) + [q(t) - q^3(t) + X(t)]h , \qquad (2.1)$$

where $X(t)$ is a random number chosen from a Gaussian distribution of mean zero and variance $\sqrt{2D/h}$. We have not retained terms of higher order in the integration step h because their effects are negligible if h is chosen to be sufficiently small. For each realization of the sequence

$X(t)$ we compute the time that it takes the process $q(t)$ starting from $q = -1$ to first arrive at $q = 0$ and to first arrive at $q = 1$.

If the noise driving Eq. (1.1) is colored then we must discretize the coupled set (1.1) and (1.4)

$$q(t+h) = q(t) + [q(t) - q^3(t) + \mu(t)]h , \qquad (2.2)$$

$$\mu(t+h) = \mu(t) + [X(t) - \mu(t)]\frac{h}{\tau} , \qquad (2.3)$$

where once again we have neglected higher-order contributions in h. Initially the value of q is -1 and the process $\mu(t)$ has a stationary Gaussian distribution. Again, for every trajectory we compute the time for the system to first reach the values $q = 0$ and $q = 1$.

In order to test the accuracy of our simulations we have in a few cases carried out a much more accurate simulation for comparison. This latter procedure, requiring much more computing time, uses a different random number generator, a smaller integration step, an improved algorithm for the integration of the equations,[21] and a greater number of trajectories (5000). The results from this more accurate simulation confirm the numbers that we report below within our estimated errors.

A different algorithm for the numerical simulation of colored noise has been reported recently by Fox *et al.*[22] This new algorithm uses an integral version of Eq. (1.4)

$$\mu(t+h) = \mu(t)e^{-h/\tau} + g(t) , \qquad (2.4)$$

where $g(t)$ is a Gaussian number of zero mean and variance $\{D[1 - \exp(-h/\tau)]/\tau\}^{1/2}$. Since Eq. (2.4) is exact even for long step sizes, we could in principle save computing time. The actual situation for a MFPT simulation, however, is not so optimistic, as is shown in Ref. 23. The boundary conditions that appear in a MFPT simulation cause a strong dependence of the result on the step size. Therefore, the step has to be sufficiently small and there is no difference between the two methods. This is clearly seen in Fig. 1, where the two algorithms are tested in the MFPT simulation for the *noise* variable to reach a prefixed value. We see that the smallness of the needed step size makes the difference between the two methods irrelevant.

III. RESULTS

A. White noise

We begin by studying the process (1.1) driven by white noise. The purpose is to test the theoretical approximations and the digital simulation in the limit in which it is possible to obtain precise numerical results from exact quadratures. In particular, we want to test the reliability of our MFPT simulation and the domain of validity of Eqs. (1.5) and (1.6).

In Fig. 2 we show the relation $T_{\text{bot}}/T_{\text{bot}}^K$, using as T_{bot} both the exact numerical integral and the simulation results. There are clearly important corrections to the Kramers time. In the range $0.1 \leq D \leq 0.2$, i.e., for relatively small values of D, the errors in the Kramers time exceed 25%. Kramer's time formula requires noise intensities smaller than 0.05 for the error to be smaller than 10%.
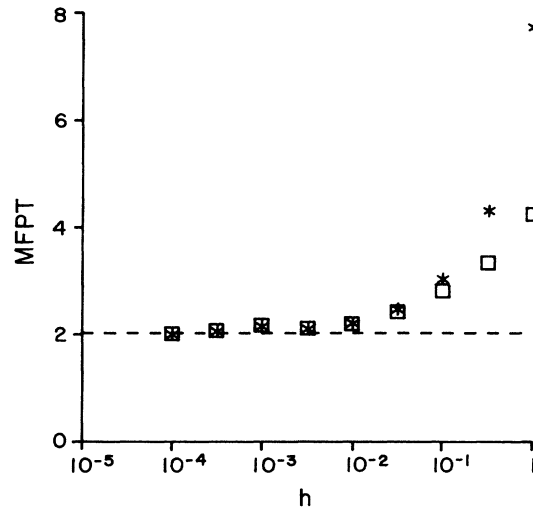

FIG. 1. MFPT results for Eq. (1.4) vs the integration step h. The noise variable $\mu(t)$ starts from $\mu = 0$ and reaches the boundary at $\mu = 0.31$. The parameters $D = 0.1$, $\tau = 1$ lead to the numerical result $T = 2.026$. Asterisks, algorithm of Fox *et al.* (Ref. 22); squares, algorithm of Eq. (2.3) (Ref. 20). The central processing unit time is nearly the same for both points of each pair.

Unfortunately, the calculation time grows exponentially with decreasing D for small D in a MFPT simulation, and it is not practical to simulate noises of intensities smaller than 0.07. The correction (1.7) of Larson and Kostin[17] improves the theoretical prediction substantially for intensities smaller than 0.2.

The assumption $T_{\text{bot}}/T_{\text{top}} = 2$ is asymptotically valid in the limit $D \to 0$. In Fig. 3 we see that the departure from this assumption for intermediate D is quite significant. The value of $T_{\text{bot}}/T_{\text{top}}$ is 2.15 for $D = 0.1$
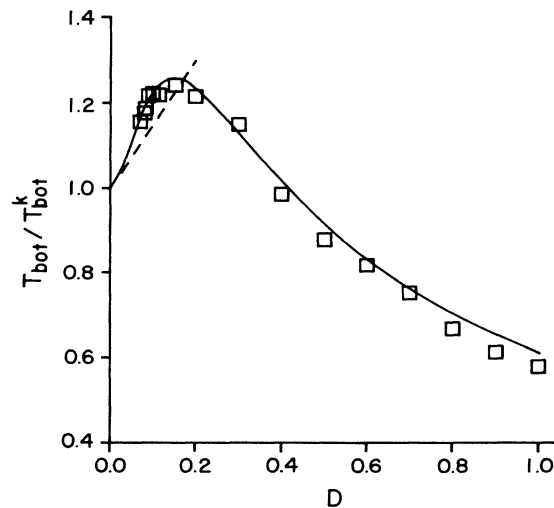

FIG. 2. $T_{\text{bot}}/T_{\text{bot}}^K$ vs D for the white-noise case. Squares, simulation; solid line, exact result; dashed line, Larson and Kostin correction (1.7).
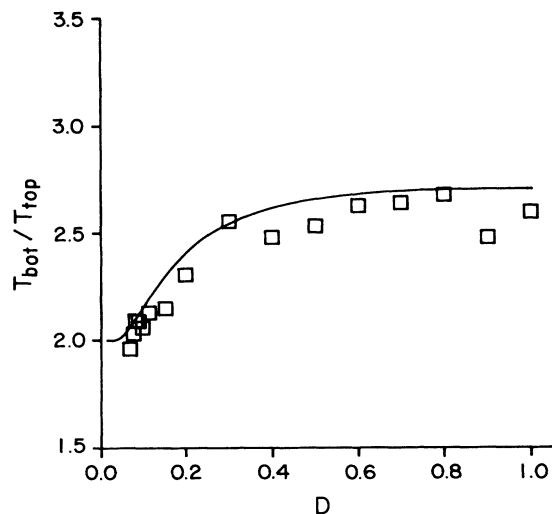
FIG. 3. T_{bot}/T_{top} vs D for the white-noise case. Squares, simulation; solid line, exact results.

FIG. 4. Simulation results for T_{bot}/T_{top} vs τ. Squares, $D=0.083$; triangles, $D=0.114$; rhombuses, $D=0.153$.

and reaches 2.7 for $D=1$.

These remarks serve to stress the fact that Eqs. (1.5) and (1.6) fail to describe accurately the properties of the MFPT for finite D. The disagreements are substantial even for the smallest D that can be implemented reasonably in a digital simulation or, which is perhaps more important, in analog experiments.[2]

Finally, the simulation of the white-noise case has been useful to test the MFPT algorithm. In Figs. 2 and 3 we see that the results of our simulation fit the exact theoretical curves reasonably well.

B. Colored noise: small τ

Since all the theories for small τ [Eqs. (1.8)–(1.12)] converge to Eqs. (1.5) and (1.6) in the limit $\tau \to 0$, the failure of these latter equations for finite D described in Sec. III A presents a new problem. If we were to compare directly the results of the small-τ theories with the ones obtained from simulations, the effects of the correlation time τ, which we are interested in, may be masked by errors introduced by small-D approximations. The way to avoid this problem is to analyze the ratio $T(\tau)/T(0)$ instead of $T(\tau)$. In this way, the errors arising from the steepest descent calculation are expected to be reduced.

The first point we wish to stress via the simulation results is the very different behavior of $T_{top}(\tau)$ and $T_{bot}(\tau)$. The comparison of the two MFPT's is plotted in Fig. 4 for the three intensities D considered. We see that T_{bot}/T_{top} has a value near 2 for $\tau \to 0$, but this ratio decreases very rapidly with τ, reaching the value 1 for moderately colored noises. This departure is of course related to the departure of the separatrix from $q=0$ with increasing τ and reflects the fact that the actual separatrix has already been crossed when $q=0$ is reached. Any assumption of a simple proportionality between $T_{bot}(\tau)$ and $T_{top}(\tau)$ is thus seen to fail for colored noise even for small values of τ.

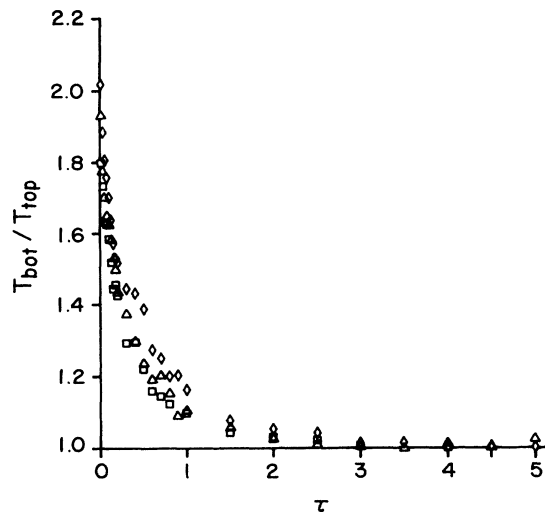The results of different theories are usually given by ex-

pressions for T_{top} or T_{sep} such as Eqs. (1.8)–(1.11) whose white-noise limit is (1.4). For the correct interpretation of the results for T_{top} one must consider two possibilities: (a) The theory gives the correct behavior for T_{top}. In that case the theory does not directly address the behavior of T_{bot}. (b) The theory gives the correct behavior for T_{bot}, i.e., one must interpret the result as $T_{bot}=2T_{top}$, T_{top} then being a function with no simple connection to the actual MFPT to reach $q=0$. This explains the existence of two different leading behaviors in τ among the theories for small τ.

The values of T_{bot} obtained from our simulations show a slope for $T_{bot}(\tau)/T_{bot}(0)$ of $\frac{3}{2}$ for very small values of τ. This is the prediction of Eqs. (1.10) and (1.12) and also of (1.8) and (1.9) if these latter two are interpreted as representing $T_{bot}/2$ (the interpretation we adopt henceforth). The results are seen in Fig. 5, where we have plot-
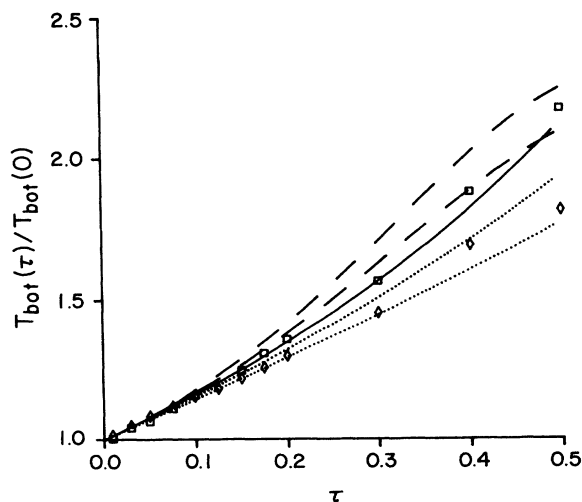

FIG. 5. $T_{bot}(\tau)/T_{bot}(0)$ vs τ. Squares, $D=0.083$; rhombuses, $D=0.153$; solid line, Eq. (1.9); dashed line, Eq. (1.10); dotted line, Eq. (1.12).

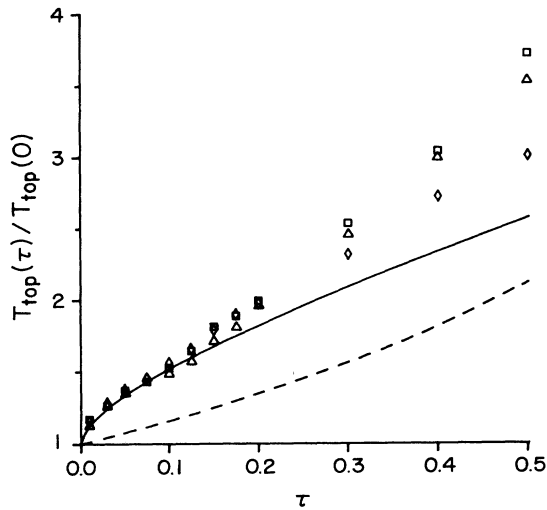FIG. 6. $T_{top}(\tau)/T_{top}(0)$ vs τ. Squares, $D = 0.083$; triangles, $D = 0.114$; rhombuses, $D = 0.153$; solid line, Eq. (1.11); dashed line, Eq. (1.9).

FIG. 7. $T_{bot}(\tau)$ vs τ. Squares, $D = 0.083$; rhombuses, $D = 0.153$; solid lines, Eq. (1.12); dashed lines, Eq. (1.14); dotted lines, Eq. (1.13).

ted Eq. (1.9) as representative of the $T_{bot} = 2T_{top}$ theories. All the theories fit the simulation data quite well for small τ. For larger τ the differences between the theories become apparent, but none of them seems to fit the simulations much better than the others. We have also plotted Eqs. (1.10) [using $T_{sep}(\tau)/T_{sep}(0)$ in this case] and (1.12) because these theories predict a D-dependent slope for $T(\tau)/T(0)$. The variation of the slope is predicted by both equations, but the actual value is underestimated by Eq. (1.12) and is overestimated by Eq. (1.10).

The plot of $T_{top}(\tau)/T_{top}(0)$ in Fig. 6 shows a distinctive small-τ curvature that is correctly predicted by Eq. (1.11) and not by the other theories. The special boundary conditions that have to be imposed, and that only the theory of Doering *et al.*[4] considers, give the new term proportional to $\sqrt{\tau}$ that leads to this curvature.

C. Colored noise: large τ

The large correlation time expressions (1.13) and (1.14) predict a MFPT that grows exponentially with $2\tau/27D$ in the limit $\tau \to \infty$. It is not possible to deal with *very* large values of τ in a MFPT simulation because the calculation time grows as its own result, i.e., exponentially. In the present simulation, with D near 0.1, the values of τ used, though perhaps not asymptotically large, give values of τ/D larger than 40, which is sufficiently large to allow comparison of the diverse large-τ theories.

This comparison is shown in Fig. 7, where we plot $T_{bot}(\tau)$ on a logarithmic scale. The plot of $T_{top}(\tau)$ is indistinguishable from that of $T_{bot}(\tau)$ for τ larger than 1.5. It follows from Fig. 7 that all the theories try to have the correct exponential behavior, but the precise values predicted for the MFPT are clearly wrong (in some cases with deviations of orders of magnitude).

These results seem to indicate that the discrepancies between the theories and the numerical results lie in the prefactors and not in the exponential dependence on τ.[14]
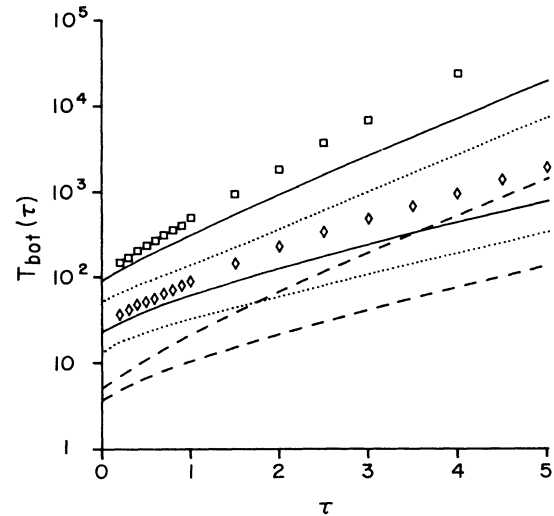
In the following, instead of trying to calculate that prefactor, we use approximate arguments to obtain a scaling law that fits the numerical results reasonably well and gives a possible dependence of the MFPT on the noise parameters τ and D.

For large values of the correlation time, the change in the noise is so slow that the analysis of the system (1.1) and (1.4) can be done from a semideterministic point of view. The dashed line in Fig. 8 represents the separatrix $\mu_{sep}(q)$ between the initial conditions that drive the system to each well. The deterministic evolution $(D = 0)$ of the two variables q and μ is shown in the figure for two values of τ.

If τ is very large, the evolution of the noisy system from a given initial condition is very similar to the deterministic evolution, and therefore the MFPT to reach the second well is related to the mean time taken by the system to reach the separatrix. In Fig. 8 a sample trajectory of the system is shown. Once the system has crossed this curve, it has a finite probability (parameter-independent to leading order) of actually reaching the second well. Therefore, the MFPT in which we are interested is likely to be proportional to the mean time to reach the separatrix. The dependence of the separatrix-crossing position on the parameters of the problem should then give the dependence of MFPT on these parameters.

This kind of reasoning is followed in Refs. 8 and 9 to obtain Eqs. (1.13) and (1.14). In the case of Eq. (1.14), the actual separatrix is replaced by the straight line $q = -1\sqrt{3}$ (vertical dotted line in Fig. 8). In the case of Eq. (1.13) the noise is considered as constant, and the actual separatrix is replaced by a critical value $\mu_c = 2/3\sqrt{3}$ (horizontal dotted line in the same figure).

The extension of the Tsironis-Grigolini[8] (TG) calculation to large but finite correlation times is discussed in Ref. 10, where it is argued that a system with the "noise" equal to the (constant) critical value μ_c requires an

infinite time to cross the inflection point $q = -1/\sqrt{3}$; it is furthermore shown that the system must typically reach values of the noise much larger than μ_c to complete the transfer from one well to the other. This larger value $\mu > \mu_c$ of the noise must depend on τ, and its lower bound μ_τ is calculated under the condition that the deterministic time to go to the other well be smaller than the correlation time τ of the noise. This lower bound for the critical value of the noise gives a correction in the exponent of order $1/\tau^2$ to the TG result.

We shall here obtain the (approximate) τ dependence of μ. We start from the TG calculation.[8] In this model one must wait a time T to let the noise reach the critical value μ_c (note that if μ were constant then μ_c *would* be the separatrix). This time is calculated by standard procedures,[15]

$$T(\mu_c) = \frac{\tau^2}{D} \int_0^{\mu_c} dy \int_{-\infty}^{y} dz \, \exp\left[-\frac{\tau}{2D}(z^2 - y^2) \right] . \quad (3.1)$$
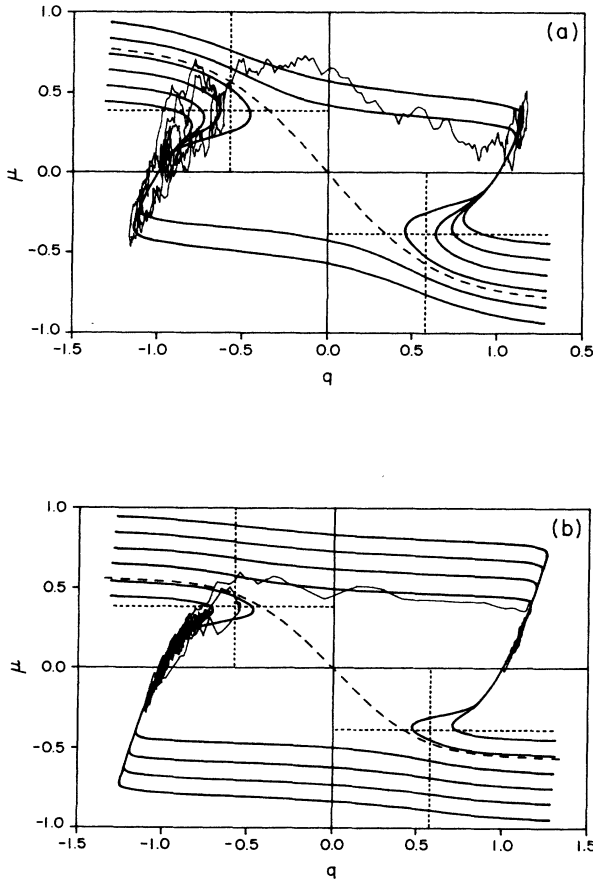
FIG. 8. Trajectories for the two variables q and μ. Solid thick lines, deterministic trajectories $(D=0)$; solid thin line, stochastic trajectory $(D=0.5)$; dashed line, actual separatrix; dotted lines, $q = \pm 1/\sqrt{3}$ and $\mu = \pm 2/3\sqrt{3}$ used as effective separatrices in the theories leading to Eqs. (1.14) and (1.13), respectively. (a) $\tau = 5$. (b) $\tau = 15$.

After some manipulation, this equation yields

$$T(\mu_c) = \tau\sqrt{\pi} \left\{ 1 + \text{erf}\left[\left[\frac{\tau}{2D} \right]^{1/2} \mu_c \right] \right\}$$

$$\times e^{(\tau/2D)\mu_c^2} F\left[\left[\frac{\tau}{2D} \right]^{1/2} \mu_c \right]$$

$$- 2\tau \int_0^{(\tau/2D)^{1/2}\mu_c} dy \, F(y) , \quad (3.2)$$

where $\text{erf}(x)$ is the error function and $F(x)$ is the Dawson Integral.[24] For large τ, the asymptotic behavior of Eq. (3.2) is

$$T(\mu_c) = \frac{\sqrt{2\pi D\tau}}{\mu_c} e^{(\tau/2D)\mu_c^2} \quad (3.3)$$

which is the TG result.[8] In view of Eqs. (3.2) and (3.3), the MFPT in the TG model is τ times a function of $\tau\mu_c^2/D$.

Let us go one step further and neglect only the white stochastic driving force in (1.4) but retain the dissipative time dependence of μ. The variable μ then experiences exponential relaxation. Retaining this feature yields behavior closer to the true evolution of the two-dimensional system. With this deterministic but time-varying-μ approximation, the slope of the separatrix at $q = 0$ is a simple function of τ as a consequence of the exponential relaxation of the "noise" variable,[9]

$$\left. \frac{d\mu_{\text{sep}}}{dq} \right|_{q=0} = -\left[1 + \frac{1}{\tau} \right] . \quad (3.4)$$

Therefore, near $q = 0$ the position of the separatrix is given by

$$\mu_{\text{sep}}(q, \tau) = \left[1 + \frac{1}{\tau} \right] \mu_{\text{sep}}(q, \infty) . \quad (3.5)$$

Although this relation is only valid close to $q = 0$, we assume the same dependence for the entire separatrix.

These arguments can be reasonably retained even in the presence of the white noise in (1.4) if τ is sufficiently large that if at a given time the system is above the separatrix, it has enough time to evolve towards the other well before the noise $\mu(t)$ departs appreciably from its deterministic exponential relaxation. Then, generalizing the ideas of Refs. 8 and 10, we take for the MFPT calculation the approximate τ-dependent critical value

$$\mu(\tau) = \left[1 + \frac{1}{\tau} \right] \mu(\infty) = \left[1 + \frac{1}{\tau} \right] \mu_c \quad (3.6)$$

which is consistent with the lower bound found in Ref. 10. As a consequence, the dependence of the MFPT on the noise parameters is

$$\frac{T}{\tau} = f\left[\frac{\tau}{D} \left[1 + \frac{1}{\tau} \right]^2 \right] . \quad (3.7)$$

This scaling law is tested in Fig. 9, where we have plotted the simulation points for τ above 0.9. For τ smaller than this value the points deviate from the behavior pre-
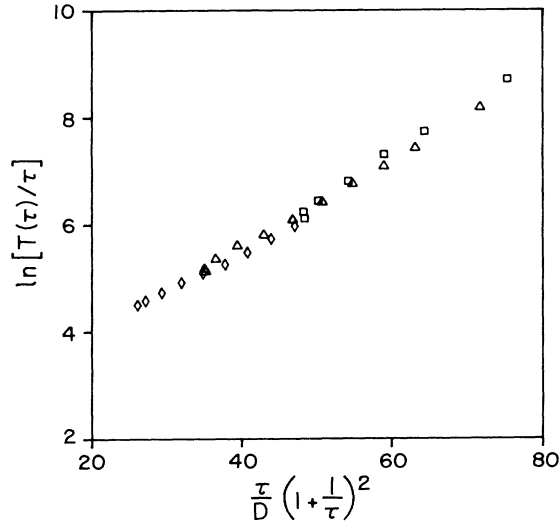
FIG. 9. $T(\tau)/\tau$ vs $(\tau/D)(1+1/\tau)^2$ for $\tau \geq 0.9$. Squares, $D = 0.083$; triangles, $D = 0.114$; rhombuses, $D = 0.153$.
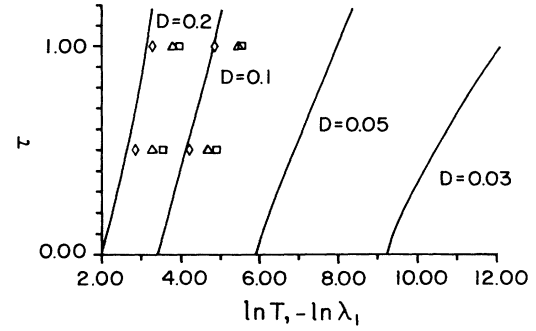

FIG. 10. $\ln\lambda_1^{-1}$ and $\ln T$ vs τ . Solid lines; numerical resutls from Ref. 9. Symbols; simulation results for $D = 0.2$ and $D = 0.1$. Squares, T_{bot} ; triangles, T_{top} ; rhombuses, $T_{bot}/2$.

precise relation (4.1) reads

$$T_{bot} = 2\lambda_1^{-1} \tag{4.2}$$

and one should bear in mind that even this relation is only valid for small D .

dicted by Eq. (3.7), as can be expected from the singularity in (3.6) at $\tau = 0$. In light of this figure, the predicted scaling is convincinly confirmed. The result (3.7) calls for more theoretical work.

IV. THE EIGENVALUES OF THE FOKKER-PLANCK EQUATION

A method frequently used to estimate the MFPT without carrying out digital or analog simulations is the numerical solution of the eigenvalue problem for the two-dimensional Fokker-Planck equation corresponding to the system (1.1), (1.4) (e.g., by using a matrix continued-fraction expansion).[11,12] The MFPT to reach the barrier is calculated as the inverse of the first nonvanishing eigenvalue λ_1 ,

$$T = \lambda_1^{-1} . \tag{4.1}$$

However, the connection between the MFPT and the eigenvalue λ_1 in a system with various attractors such as ours is only clear under certain conditions.[25] First, one must be in the weak-noise limit. Second, the probability of turning back to the first attractor (the first well) without reaching the second one, once the system has crossed the boundary condition of the MFPT, must be small. This second condition clearly does not hold for the boundary condition at $q = 0$ because the probability of turning back once the system reaches the top of the barrier is not necessarily small (it is equal to $\frac{1}{2}$ for white noise). However, the condition holds for the boundary at $q = 1$ because the crossing of the boundary means that the second well has been reached.

The eigenvalue λ_1 is therefore in general related to the MFPT T_{bot} and not to T_{top} . This conclusion is tested in Fig. 10, where T_{top} and T_{bot} are compared with the numerical eigenvalue results of Ref. 12. It can be seen there that the inverse of the eigenvalue λ_1 coincides for small D with half of the MFPT T_{bot} and not with T_{top} . Thus the

V. CONCLUSIONS

The main conclusions of this paper can be summarized as follows:

(a) Kramers's formulas (1.5) and (1.6) and their correction (1.7) by Larson and Kostin are asymptotic results. In the experimentally accessible range of variables further corrections to these results become important. Hence these formulas cannot be used to conclude the validity of numerical or digital simulations.

(b) T_{bot} and T_{top} are neither equivalent nor are they in general related in a simple universal way; they contain different physical information. Therefore one of these quantities cannot in general be used to deduce the behavior of the other. T_{bot} is the more physically relevant time and is rather insensitive to the precise location of the initial and final values so long as they are both deep within their respective wells.

(c) At present only the small-τ case $(\tau < 0.3)$ is explained satisfactorily by the theories. All existing small-τ theories for T_{bot} and T_{sep} yield an initial slope of $\frac{3}{2}$, which is clearly the behavior also observed in numerical simulations. The differences between (1.8), (1.10) (in both of which the $3\tau/2$ arises from the prefactor, and (1.9) (where it arises in the exponent) are not apparent in the range $\tau < 0.2$. Therefore all the theories are equivalent from a practical point of view in this range. It is not possible to conclude which theory leads to the most accurate D dependence that becomes evident in the large-τ simulations $(0.2 < \tau < 1)$.

(d) Simulations of T_{top} for small τ clearly confirm the $\sqrt{\tau}$ contribution found by Doering *et al.* in (1.11).

(e) The large-τ case is explained only qualitatively by current theories; there remain large quantitative differences between the theories and the results of numerical simulations. For very large values of τ the fluctuating potential picture of Tsironis and Grigolini[8] yields the correct asymptotic exponential dependence on $2\tau/27D$ in

the MFPT. Corrections to the asymptotic exponent can be obtained by a simple extension of the fluctuating potential idea, cf. Eqs. (3.6) and (3.7). Nevertheless there are serious quantitative disagreements with the simulations that arise from prefactor contributions that have not been properly captured.

(f) The dominant eigenvalue of the two-variable (q,μ) Fokker-Planck equation should be identified with T_{bot} through Eq. (4.2) for small D.[19]

*Present and permanent address: Fermi National Accelerator Laboratory, Batavia, Illinois 60510.

[1]P. Hänggi, F. Marchesoni, and P. Grigolini, Z. Phys. B **56**, 333 (1984).

[2]P. Hänggi, T. J. Mroczkowski, F. Moss, and P. V. E. McClintock, Phys. Rev. A **32**, 695 (1985).

[3]J. Masoliver, B. J. West, and K. Lindenberg, Phys. Rev. A **35**, 3086 (1987).

[4]C. R. Doering, P. S. Hagan, and C. D. Levermore, Phys. Rev. Lett. **59**, 2129 (1987).

[5]R. F. Fox, Phys. Rev. A **37**, 911 (1988).

[6]M. M. Klosek-Dygas, B. J. Matkowsky, and Z. Schuss, Phys. Rev. A **38**, 2605 (1988).

[7]J. F. Luciani and A. D. Verga, J. Stat. Phys. **50**, 567 (1988).

[8]G. P. Tsironis and P. Grigolini, Phys. Rev. Lett. **61**, 7 (1988); G. P. Tsironis and P. Grigolini, Phys. Rev. A **38**, 3749 (1988).

[9]P. Hänggi, P. Jung, and F. Marchesoni, J. Stat. Phys. (to be published).

[10]F. J. de la Rubia, E. Peacock-López, G. P. Tsironis, K. Lindenberg, L. Ramirez-Piscina, and J. M. Sancho, Phys. Rev. A **38**, 3827 (1988)

[11]P. Jung and H. Risken, Z. Phys. B **61**, 367 (1985).

[12]P. Jung and P. Hänggi, Phys. Rev. Lett. **61**, 11 (1988).

[13]R. Mannella and V. Palleschi, Phys. Lett. **A129**, 317 (1988).

[14]R. Mannella and V. Palleschi, Phys. Rev. A **39**, 3751 (1989).

[15]C. W. Gardiner, *Handbook of Stochastic Methods* (Springer-Verlag, Berlin, 1983).

[16]H. A. Kramers, Physica **7**, 284 (1940).

[17]R. S. Larson and M. D. Kostin, J. Chem. Phys. **69**, 4821 (1978).

[18]P. Hänggi, P. Jung, and P. Talkner, Phys. Rev. Lett. **60**, 2804 (1988).

[19]C. R. Doering, R. J. Bagley, P. S. Hagan, and C. D. Levermore, Phys. Rev. Lett. **60**, 2805 (1988).

[20]J. M. Sancho, M. San Miguel, S. L. Katz, and J. D. Gunton, Phys. Rev. A **26**, 1589 (1982).

[21]W. Rumelin, SIAM J. Numer. Anal. **19**, 604 (1982).

[22]R. F. Fox, I. R. Gatland, R. Roy, and G. Vemuri, Phys. Rev. A **38**, 5938 (1988).

[23]W. Strittmatter (unpublished).

[24]*Handbook of Mathematical Functions*, edited by M. Abramowitz and I. A. Stegun (Dover, New York, 1965).

[25]P. Talkner, Z. Phys. B **68**, 201 (1987).